White Rose Research Online

eprints@whiterose.ac.uk
https://eprints.whiterose.ac.uk
Universities of Leeds, Sheffield and York

Deposited via The University of Sheffield.

White Rose Research Online URL for this paper:
https://eprints.whiterose.ac.uk/id/eprint/174982/

Version: Accepted Version

Proceedings Paper:
Dedeoglu, S., Konstantopoulos, G.C. and Komurcugil, H. (2021) Current-limiting VSG for renewable energy applications. In: Proceedings of 2021 IEEE 30th International Symposium on Industrial Electronics (ISIE). 2021 IEEE 30th International Symposium on Industrial Electronics (ISIE), 20-23 Jun 2021, Virtual conference (Kyoto, Japan). Institute of Electrical and Electronics Engineers. ISBN: 9781728190242. ISSN: 2163-5137. EISSN: 2163-5145.

https://doi.org/10.1109/ISIE45552.2021.9576298

© 2021 IEEE. Personal use of this material is permitted. Permission from IEEE must be obtained for all other users, including reprinting/ republishing this material for advertising or promotional purposes, creating new collective works for resale or redistribution to servers or lists, or reuse of any copyrighted components of this work in other works. Reproduced in accordance with the publisher's self-archiving policy.

Reuse
Items deposited in White Rose Research Online are protected by copyright, with all rights reserved unless indicated otherwise. They may be downloaded and/or printed for private study, or other acts as permitted by national copyright laws. The publisher or other rights holders may allow further reproduction and re-use of the full text version. This is indicated by the licence information on the White Rose Research Online record for the item.

Takedown
If you consider content in White Rose Research Online to be in breach of UK law, please notify us by emailing eprints@whiterose.ac.uk including the URL of the record and the reason for the withdrawal request.

UNIVERSITY OF LEEDS
University of Sheffield
UNIVERSITY of York

Current-Limiting VSG for Renewable Energy Applications

Seyfullah Dedeoglu[1], George C. Konstantopoulos[2], and Hasan Komurcugil[3]

[1]Dept. of Automatic Control and Systems Engineering, The University of Sheffield, Sheffield, S1 3JD, UK

[2]Dept. of Electrical and Computer Engineering, University of Patras, 26504 Rio, Patras, Greece

[3]Dept. of Computer Engineering, Eastern Mediterranean University, Famagusta, Via Mersin 10, Turkey

Email: sdedeoglu1@sheffield.ac.uk, g.konstantopoulos@ece.upatras.gr, hasan.komurcugil@emu.edu.tr

***Abstract*—In this paper, an improved nonlinear controller structure, which inherits both virtual inertia (VI) and current-limiting properties in grid-connected voltage-source converters (VSCs), is proposed. The proposed method inherits the $V_{dc} \sim \omega$ droop control for inertia emulation and frequency control, and $Q \sim V$ droop control for AC voltage support. The current-limiting property, which is a critical issue for the protection of grid interface inverters throughout the whole operation including the grid faults is proven analytically for VI-based VSCs using nonlinear control theory. Furthermore, small-signal stability of the system is examined considering the effects of different controller gains in order to provide guidance for the selection of their values. To validate both the small-signal stability and nonlinear current limitation proof, extensive Matlab/Simulink simulations are performed.**

***Index Terms*—Nonlinear droop control, virtual synchronous control, current-limiting property, DC-link voltage control, voltage-source converter, stability analysis.**

I. Introduction

It is an indisputable fact that the way the energy has been produced for centuries should be modified to decrease the detrimental effects of greenhouse gases on climate change. The best way to realize this modification is to modernize the traditional power grid by making use of environmentally friendly distributed energy resources (DERs) such as wind turbine generators and photovoltaics [1]–[3]. The integration of DERs to the utility grid is achieved via power interface devices such as voltage-source converters (VSCs) equipped with intelligent control strategies. The control strategies should ensure the synchronization with the utility grid, accurate power control, voltage and frequency regulation to form a reliable operation of the individual DERs and the network [4]–[6].

The power and control system societies unite on the idea of using the well-known droop controllers to achieve the control tasks mentioned above. Droop controllers have many advantages such as being able to work without communication networks, provide accurate power sharing, and realize voltage and frequency regulations in traditional synchronous generator (SG) based grid systems. However, they are oversensitive against the disturbances such as system parameter and weather condition changes, and have slow and poor dynamic performances in renewable energy (RE) applications [7], [8]. Besides, conventional droop methods are designed assuming the output impedances are inductive, which is an invalid assumption in low power and RE applications and can lead to inaccurate power sharing, poor voltage and frequency control and eventually the instability of the system [7]. In [9] and [10], a universal droop control and an exponential function based droop control have been proposed, respectively to deal with those problems.

In general, the priority in converter-based RE applications is to send the maximum power to the grid without considering the inertia requirements, which are critical for energy balance and system stability, dictated by the grid authorities [11]. However, even if providing inertia in RE applications is not a strictly applied requirement in some countries since a high percentage of energy production depends on SG-based sources in current operations, inertia will be one of the key-enablers to increase the proportion of RE-based energy production in the future [12], [13]. As the majority of RE sources are not capable of providing physical inertia, VI concept has been first proposed in [14] for power electronic converters and its various modifications such as synchronverters, virtual oscillator control and inducverters have been published to deal with this problem [15]. Generally, the current VI algorithms assume either constant or quasi-constant dc-link voltage, which may work well for some specific applications, but may not be always guaranteed due to the intermittent nature of the RE sources. This issue is examined in [11], [16] by controlling the DC-link capacitor voltage for both inertia emulation and synchronization purposes.

Furthermore, since the operation of power converters is achieved using semiconductor switches, which can be vulnerable especially in sudden abnormal situations, such as grid faults, the control algorithms should ensure that the critical system states, such as system currents, will stay in the defined limits to guarantee a reliable operation. In conventional applications, either saturated PI controllers are employed in inner loops or controller algorithm modification is realized. However, those methods may lead to integrator wind-up and latch-up in the aggressive transient cases, cause a possible loss

This work is supported by EPSRC under Grants No EP/S001107/1 and EP/S031863/1, and under Grant 81359 from the Research Committee of the University of Patras via "C. CARATHEODORY" program.

978-1-7281-9023-5/21/$31.00 ©2021 IEEE

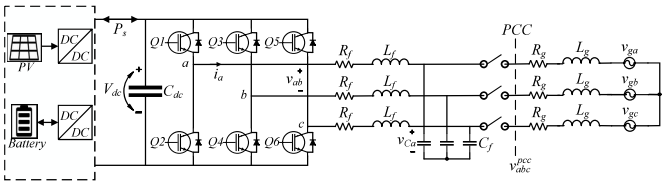

Fig. 1. DER-sourced grid-connected VSC system

of system stability and damage to the power converter device [17], [18]. To address this issue, a nonlinear droop control method, which can analytically prove the current-limiting property independently from the system parameters unlike [19], has been proposed in [20] for single-phase inverters and in [21] for three-phase rectifiers. However, the applicability of this method for VI applications has not been proven, yet.

Hence, in this paper, an improved nonlinear control method for DER-sourced grid-connected VSCs is proposed. This approach ensures the VSC current limitation at all times even under grid faults using nonlinear control theory and utilizes the recently proposed virtual synchronous control (ViSynC) [11] to provide virtual inertia to the system when needed. Unlike [11], which uses saturated PI controllers in the control loops and cannot guarantee the current-limiting property and system stability at all times, in the proposed method, the current-limiting property is analytically proven for the first time for VI-based inverters through nonlinear control theory using the recently introduced state-limiting PI controller [22]. Furthermore, closed-loop stability is examined via small-signal system analysis and useful root-locus plots by altering the controller gains are provided to guide the prospective users. To prove the effectiveness of the proposed method, extensive simulation results are presented.

II. Dynamic System Modeling and Necessary Definitions

The system under consideration is a DER-sourced VSC connected to a point of common coupling (PCC) via an LC filter, as depicted in Fig. 1. The filter parasitic resistance, inductance, and capacitor are described as R_f, L_f, C_f, respectively, while the line between the PCC and the main grid has a resistance R_g and an inductance L_g. The DC side of the inverter is modeled as a bidirectional power source unlike [11], which has a unidirectional power source, while V_{dc} and C_{dc} denote dc-link voltage and capacitor. Following the analysis from [23], the three phase balanced PCC natural frame voltages, RMS voltage and phase angle are taken as v_{abc}^{pcc}, V_{rms}, and θ_g, respectively. By utilizing the clockwise axis transformation from [24], and considering the global dq frame PCC voltages as $V_d^{pcc} = \sqrt{2}V_{rms}$ and $V_q^{pcc} = 0$ as in [11], the local dq frame PCC voltages are computed as

$$\begin{bmatrix} V_{dl}^{pcc} \\ V_{ql}^{pcc} \end{bmatrix} = \begin{bmatrix} V_d^{pcc}\cos\delta \\ -V_d^{pcc}\sin\delta \end{bmatrix}, \tag{1}$$

where $\delta = \theta - \theta_g$ denotes the phase angle subtraction between the VSC and the PCC. Then, the VSC dynamics in the local dq frame are given as

$$L_f\frac{di_d}{dt} = -R_f i_d + \omega L_f i_q - V_{dl}^{pcc} + V_d \tag{2}$$

$$L_f\frac{di_q}{dt} = -R_f i_q - \omega L_f i_d - V_{ql}^{pcc} + V_q \tag{3}$$

where i_d, i_q and V_d, V_q stand for the local dq frame VSC currents and voltages, whereas $\omega = \dot{\theta}$ is the angular frequency of the VSC, which will be defined in the next section to provide virtual inertia. Thus, considering (1) and local frame VSC currents, the VSC active and reactive power can be expressed as

$$\begin{aligned} P &= \frac{3}{\sqrt{2}}V_{rms}i_d\cos\delta \\ Q &= -\frac{3}{\sqrt{2}}V_{rms}i_d\sin\delta. \end{aligned} \tag{4}$$

Since the power equations (4) consist of nonlinear terms, any control approach including the well-known droop control will lead to a nonlinear closed-loop system, which makes the stable and reliable operation a difficult task to achieve, especially under the faulty grid cases. To this end, the main task in this paper is to design a control method, which implements a $Q \sim V$ droop function and guarantee current limitation via nonlinear theory under both normal and faulty grid cases, while also providing inertia support via formulating a relationship between the DC-link voltage and AC frequency.

III. Proposed Nonlinear Current-Limiting Controller and ViSynC Integration

A. Proposed Nonlinear Controller

In order to achieve the inherent current-limiting property with a simple controller structure, the proposed method aligns the inverter current to the local d axis, i.e. q axis current is zero, then uses state-limiting PI controller [22] with required bounds to dynamically limit the d axis inverter current as done in [23]. However, the proposed method ensures the system stability and current limitation without assuming a constant DC-link voltage as in [23] by dynamically controlling the DC-link voltage to provide virtual inertia. For achieving those tasks, the local inverter voltages (V_d and V_q) are taken as control inputs to the system and designed as

$$V_d = V_{dl}^{pcc} + E_{max}\sin\sigma - r_v i_d - \omega L_f i_q \tag{5}$$

$$V_q = V_{ql}^{pcc} - r_v i_q + \omega L_f i_d \tag{6}$$

where E_{max} and r_v define a virtual voltage and virtual resistor being the controller parameters, σ is the controller state, $\omega L_f i_d$ and $\omega L_f i_q$ are decoupling terms. Inspired by the state-limiting PI controller [22], the controller state σ is designed as

$$\dot{\sigma} = \frac{c}{E_{max}}\left[(E^* - V_{rms}) - n(Q - Q_{set})\right]\cos\sigma \tag{7}$$

where c is the integral gain. By choosing the initial condition of the controller state σ as $\sigma_0 \in [-\frac{\pi}{2}, \frac{\pi}{2}]$ and following the analysis provided in [22], both the controller state limitation ($\sigma(t) \in [-\frac{\pi}{2}, \frac{\pi}{2}]\ \forall t \geq 0$) and anti-windup property are ensured with no oscillatory behavior in the system. Note

that when the expression $(E^* - V_{rms}) - n(Q - Q_{set})$ is regulated to zero at the steady-state, $Q \sim V$ droop control is achieved. In the droop function, E^* defines the nominal RMS grid voltage, V_{rms} is the PCC RMS voltage calculated as $V_{rms} = \sqrt{\frac{(V_{dl}^{pcc})^2+(V_{ql}^{pcc})^2}{2}}$, Q_{set} and n are the reactive power reference value and the reactive power droop coefficient, respectively.

B. ViSynC Integration

In order to obtain the angular frequency θ, which is needed for dq transformations, in this part, $V_{dc} \sim \omega$ droop dynamics are given adopting the scheme proposed in [11]. After replacing the inverter active power dynamics (4), the DC-link voltage and inverter angular frequency dynamics become

$$\frac{d}{dt}V_{dc}^2 = \frac{2P_s - 3\sqrt{2}V_{rms}i_d\cos\delta}{C_{dc}} \tag{8}$$

$$\frac{d}{dt}\omega = \frac{2P_s - 3\sqrt{2}V_{rms}i_d\cos\delta}{C_{dc}K_J} + \frac{K_T({V_{dc}}^2 - {V_{dcref}}^2) + K_D(\omega_g - \omega)}{K_J} \tag{9}$$

where P_s is injected power from the DERs, ω_g is the nominal angular frequency, K_T, K_J, and K_D are DC-link voltage tracking, inertia emulation, and damping coefficients, respectively. More information about ViSynC can be found in [11].

IV. Closed-Loop Stability Analysis

A. Current-limiting Property

Employing the proposed controller (5)-(6) dynamics into the VSC dynamics (2)-(3), the closed-loop system current dynamics can be formed as

$$L_f\frac{di_d}{dt} = -(R_f + r_v)i_d + E_{max}\sin\sigma \tag{10}$$

$$L_f\frac{di_q}{dt} = -(R_f + r_v)i_q \tag{11}$$

As it is clear from (11), if initially $i_q(0) = 0$ then $i_q(t) = 0, \forall t \geq 0$ resulting the solution $i_q(t) = i_q(0)e^{-\frac{(R_f+r_v)}{L_f}t}$. Thus, the desired current-limiting property can be achieved by guaranteeing only the d axis current will stay below a defined maximum value I_{max}. This property can be proven using the following energy-like Lyapunov function candidate [25]

$$V = \frac{1}{2}L_f i_d^2. \tag{12}$$

The time derivative of (12) by replacing (10) becomes

$$\begin{aligned}\dot{V} &= -(R_f + r_v)i_d^2 + E_{max}i_d\sin\sigma \\ &\leq -(R_f + r_v)|i_d^2| + E_{max}|i_d|.\end{aligned} \tag{13}$$

Then, (13) can be arranged as

$$\dot{V} \leq -R_f i_d^2,\ \forall\ |i_d| \geq \frac{E_{max}}{r_v} \tag{14}$$

According to (14) based on [26], the solution $i_d(t)$ is ultimately bounded, thus every solution, which initially starts with the initial condition satisfying $|i_d(0)| \leq \frac{E_{max}}{r_v}$, will stay in this range for all times. That is,

$$|i_d(t)| \leq \frac{E_{max}}{r_v}, \forall t \geq 0. \tag{15}$$

After selecting the controller parameter $E_{max} = r_v I_{max}$, where I_{max} is a given maximum current value, (15) can be written as

$$|i_d(t)| \leq I_{max}, \forall t \geq 0, \tag{16}$$

which completes the proof of the desired current-limiting property.

B. Small-signal Stability Analysis

The current-limiting property for the VI-based VSCs is proven using nonlinear control theory in the previous section. However, the entire system stability has not been examined, yet. Thus, in this section, small signal stability of VSCs equipped with the proposed nonlinear controller is analyzed. As it is proven that the q axis current will asymptotically converge to zero using the controller (6), (11) can be omitted from the system analysis for simplicity. Considering (7)-(10) and $\dot{\delta} = \omega - \omega_g = \Delta\omega$, the closed-loop system state vector becomes $x = [i_d\ \sigma\ V_{dc}^2\ \omega\ \delta]^T$. In order to examine the behavior of the entire system via root-locus analysis, the equilibrium vector can be constructed, by linearizing (4) and solving the equations (7)-(10), as $x_e = [i_{de}\ \sigma_e\ V_{dce}^2\ \omega_e\ \delta_e]^T$, where $\sigma_e \in (-\frac{\pi}{2}, \frac{\pi}{2})$. Then, the Jacobian matrix of the closed-loop system becomes (17). As a result, the closed-loop system will be asymptotically stable, if all eigenvalues of the Jacobian matrix (17) have negative real parts.

$$J = \begin{bmatrix} -\frac{(r_v+R_f)}{L_f} & \frac{E_{max}\cos\sigma_e}{L_f} & 0 & 0 & 0 \\ A\sin\delta_e & 0 & 0 & 0 & A\,i_{de}\cos\delta_e \\ -B\cos\delta_e & 0 & 0 & 0 & B\,i_{de}\sin\delta_e \\ -\frac{B\cos\delta_e}{K_j} & 0 & \frac{K_T}{K_J} & -\frac{K_D}{K_J} & \frac{B\,i_{de}\sin\delta_e}{K_j} \\ 0 & 0 & 0 & 1 & 0 \end{bmatrix} \tag{17}$$

The notations A and B in (17) are given as $\frac{3\sqrt{2}cnV_{rms}\cos\sigma_e}{2E_{max}}$ and $\frac{3\sqrt{2}V_{rms}}{C_{dc}}$, respectively. In Fig. 2, the closed-loop eigenvalue spectrum analysis is realized by adjusting the damping gain K_D between 500 and 3000, the inertia emulation gain K_J between 5 and 20, the DC voltage tracking gain K_T between 0.2 and 10, and the integral gain c between 100 and 10000 using the system and controller parameters given in Table I. The numbers and arrows in Fig. 2 define the system poles and their directions (either left or right parts of the complex plane with respect to zero) as the controller gains change. For example, while increasing K_D moves the lightly damped poles (2 and 3) towards the left direction on the complex plane, increasing K_J, K_T, and c moves them towards the right direction on the complex plane. Thus, the effectiveness and small-signal stability margins of the proposed controller are proven for broad ranges of the controller gains, which can give clear guidance to the prospective users for their applications.

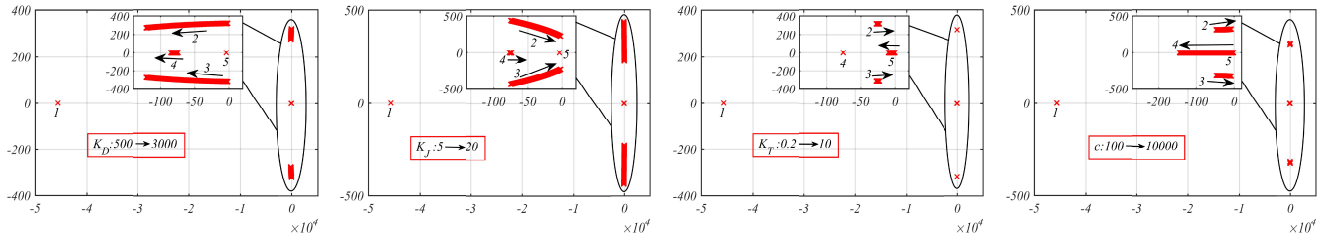

(a) (b) (c) (d)

Fig. 2. Closed-loop eigenvalue spectrum as a function of K_D (a), K_J (b), K_T (c), and c (d)

TABLE I
SYSTEM AND CONTROLLER PARAMETERS

Parameters	Values	Parameters	Values
L_f, L_g	$2.2mH$	S_{max}	990VA
R_f, R_g	0.5Ω	r_v	100Ω
n	0.011	C_{dc}	$1mF$
ω_g	$2\pi 50$	V_{dcref}	$350V$
c	5000	E^*	$110V$
I_{max}	$4.24A$	K_T	4
K_j	10	K_D	1000

V. Simulation Results for Controller Verification

In order to verify the proposed controller performance, a DER-sourced VSC connected to the grid via an LC filter and a line, as shown in Fig. 1, is simulated in the Matlab/Simulink software environment. The system and controller parameters used in the simulations are given in Table I. During the whole operation, the $Q \sim V$ droop control is enabled, and the nominal grid frequency is used. Initially, the DER power P_s is set to 400W and the reactive power set value Q_{set} is taken as 300Var. At $t = 3s$, P_s is increased to 800W, while Q_{set} is kept as 300Var. To emphasize the bidirectional operation of the VSC, at $t = 7s$, P_s is changed to -500W, which is the case the DER demands power from the VSC, and at $t = 11s$, P_s is set to 600W. At $t = 15s$, Q_{set} is increased to 500Var to prove the ability of the VSC to provide more reactive power when required. As can be seen in Fig. 3a, the proposed controller regulates the inverter active power to almost equal values of DER power P_s. Since the $Q \sim V$ droop operation is enabled, the inverter reactive power is regulated to a lower steady-state value, which can be computed as $\frac{E^* - V_{rms}}{n} + Q_{set}$ to keep the RMS voltage close to its rated value. The RMS voltage is provided, in Fig. 3d, to confirm the steady-state Q values for every operation point change.

To validate the proposed current-limiting property, at $t = 19s$, a $40V$ grid voltage drop is implemented as shown in Fig. 3d, and at $t = 20s$, the grid voltage is recovered. As it is clear in Fig. 3b, the d axis current goes to its maximum value I_{max}, while q axis current is kept as zero, which justifies the nonlinear current-limiting proof provided in the previous section. Besides, the system recovery after the fault is completed almost instantly, thus, the proposed controller inherently solves the integrator wind-up problem. In addition, the DC-link voltage is controlled very close to its reference value, even in the transients, to avoid any potential protection trip, as shown in Fig. 3c. The high frequency transients, which exist in Figs. 3a and 3c, can be removed by increasing the damping gain K_D as shown in Fig. 2.

VI. Conclusions

In this paper, an improved nonlinear controller is proposed for DER-sourced grid-connected VSCs. The proposed scheme uses DC-link voltage dynamics for inertia emulation and guarantees the reliable operation under the balanced grid faults by limiting the inverter current. The current-limiting property is analytically proven via nonlinear control theory without using any saturation units or adaptive scheme, even under the system transients, for the first time for VI-based VSCs. Moreover, the entire system stability is investigated through small-signal analysis. The effectiveness of the proposed approach is verified with comprehensive simulation results.

Future studies will investigate the performance of the proposed controller for unbalanced and short circuit grid fault cases.

References

[1] H. Farhangi, "The path of the smart grid," *IEEE Power and Energy Magazine*, vol. 8, no. 1, pp. 18-28, January-February 2010, doi: 10.1109/MPE.2009.934876.

[2] B. Kroposki et al., "Achieving a 100% Renewable Grid: Operating Electric Power Systems with Extremely High Levels of Variable Renewable Energy," *IEEE Power and Energy Magazine*, vol. 15, no. 2, pp. 61-73, March-April 2017, doi: 10.1109/MPE.2016.2637122.

[3] S. Massoud Amin and B. F. Wollenberg, "Toward a smart grid: power delivery for the 21st century," *IEEE Power and Energy Magazine*, vol. 3, no. 5, pp. 34-41, Sept.-Oct. 2005, doi: 10.1109/MPAE.2005.1507024.

[4] L. Huang, H. Xin, Z. Wang, L. Zhang, K. Wu and J. Hu, "Transient Stability Analysis and Control Design of Droop-Controlled Voltage Source Converters Considering Current Limitation," *IEEE Transactions on Smart Grid*, vol. 10, no. 1, pp. 578-591, Jan. 2019, doi: 10.1109/TSG.2017.2749259.

[5] D. Pan, X. Wang, F. Liu and R. Shi, "Transient Stability of Voltage-Source Converters With Grid-Forming Control: A Design-Oriented Study," *IEEE Journal of Emerging and Selected Topics in Power Electronics*, vol. 8, no. 2, pp. 1019-1033, June 2020, doi: 10.1109/JESTPE.2019.2946310.

[6] Y. Huang, X. Yuan, J. Hu and P. Zhou, "Modeling of VSC Connected to Weak Grid for Stability Analysis of DC-Link Voltage Control," *IEEE Journal of Emerging and Selected Topics in Power Electronics*, vol. 3, no. 4, pp. 1193-1204, Dec. 2015, doi: 10.1109/JESTPE.2015.2423494.

[7] U. B. Tayab, M. A. Bin Roslan, L. J. Hwai, and M. Kashif, "A Review of Droop Control Techniques for Microgrid," *Renewable and Sustainable Energy Reviews*, vol. 76, no. November 2016, pp. 717–727, 2017, doi: 10.1016/j.rser.2017.03.028.

[8] E. Planas, A. Gil-De-Muro, J. Andreu, I. Kortabarria, and I. Martínez De Alegría, "General Aspects, Hierarchical Controls and Droop Methods in Microgrids: A Review," *Renewable and Sustainable Energy Reviews*, vol. 17, pp. 147–159, 2013, doi: 10.1016/j.rser.2012.09.032.

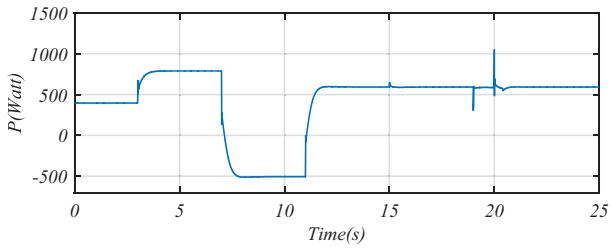

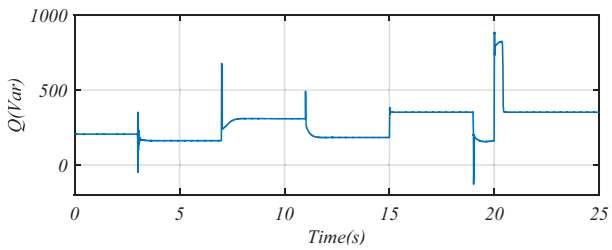

(a) Active and reactive power

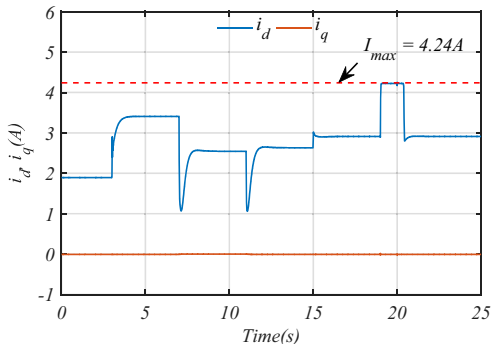

(b) Inverter i_d and iq currents

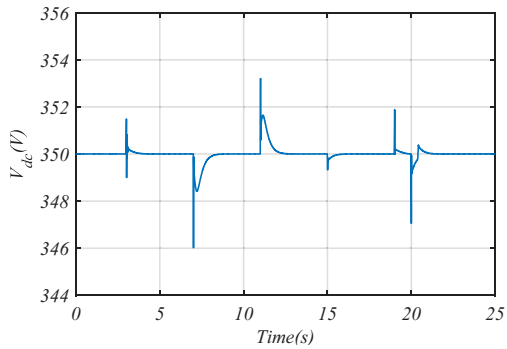

(c) DC-link voltage

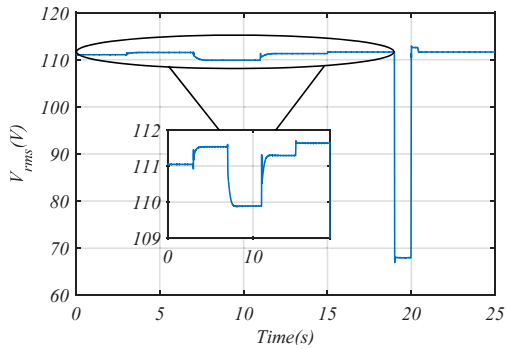

(d) RMS voltage

Fig. 3. VSC response equipped with the proposed controller.

[9] Q. Zhong and Y. Zeng, "Universal Droop Control of Inverters With Different Types of Output Impedance," *IEEE Access*, vol. 4, pp. 702-712, 2016, doi: 10.1109/ACCESS.2016.2526616.

[10] R. Wang, Q. Sun, Y. Gui and D. Ma, "Exponential-Function-Based Droop Control for Islanded Microgrids," *Journal of Modern Power Systems and Clean Energy*, vol. 7, no. 4, pp. 899-912, July 2019, doi: 10.1007/s40565-019-0544-3.

[11] L. Huang et al., "A Virtual Synchronous Control for Voltage-Source Converters Utilizing Dynamics of DC-Link Capacitor to Realize Self-Synchronization," *IEEE Journal of Emerging and Selected Topics in Power Electronics*, vol. 5, no. 4, pp. 1565-1577, Dec. 2017, doi: 10.1109/JESTPE.2017.2740424.

[12] T. Ackermann, T. Prevost, V. Vittal, A. J. Roscoe, J. Matevosyan and N. Miller, "Paving the Way: A Future Without Inertia Is Closer Than You Think," *IEEE Power and Energy Magazine*, vol. 15, no. 6, pp. 61-69, Nov.-Dec. 2017, doi: 10.1109/MPE.2017.2729138.

[13] K. S. Ratnam, K. Palanisamy, and G. Yang, "Future Low-Inertia Power Systems: Requirements, Issues, and Solutions - A Review," *Renewable and Sustainable Energy Reviews*, vol. 124, no. February, 2020, doi: 10.1016/j.rser.2020.109773.

[14] H. Beck and R. Hesse, "Virtual synchronous machine," *2007 9th International Conference on Electrical Power Quality and Utilisation*, Barcelona, 2007, pp. 1-6, doi: 10.1109/EPQU.2007.4424220.

[15] U. Tamrakar, D. Shrestha, M. Maharjan, B. Bhattarai, T. Hansen, and R. Tonkoski, "Virtual Inertia: Current Trends and Future Directions," *Applied Sciences*, vol. 7, no. 7, p. 654, 2017, doi: 10.3390/app7070654.

[16] L. Huang, H. Xin, H. Yang, Z. Wang and H. Xie, "Interconnecting Very Weak AC Systems by Multiterminal VSC-HVDC Links With a Unified Virtual Synchronous Control," *IEEE Journal of Emerging and Selected Topics in Power Electronics*, vol. 6, no. 3, pp. 1041-1053, Sept. 2018, doi: 10.1109/JESTPE.2018.2825391.

[17] A. D. Paquette and D. M. Divan, "Virtual Impedance Current Limiting for Inverters in Microgrids With Synchronous Generators," *IEEE Transactions on Industry Applications*, vol. 51, no. 2, pp. 1630-1638, March-April 2015, doi: 10.1109/TIA.2014.2345877.

[18] N. Bottrell and T. C. Green, "Comparison of Current-Limiting Strategies During Fault Ride-Through of Inverters to Prevent Latch-Up and Wind-Up," *IEEE Transactions on Power Electronics*, vol. 29, no. 7, pp. 3786-3797, July 2014, doi: 10.1109/TPEL.2013.2279162.

[19] D. Groß and F. Dörfler, "Projected grid-forming control for current-limiting of power converters," *2019 57th Annual Allerton Conference on Communication, Control, and Computing (Allerton)*, Monticello, IL, USA, 2019, pp. 326-333, doi: 10.1109/ALLERTON.2019.8919856.

[20] Q. Zhong and G. C. Konstantopoulos, "Current-Limiting Droop Control of Grid-Connected Inverters," *IEEE Transactions on Industrial Electronics*, vol. 64, no. 7, pp. 5963-5973, July 2017, doi: 10.1109/TIE.2016.2622402.

[21] Q. Zhong and G. C. Konstantopoulos, "Current-Limiting Three-Phase Rectifiers," *IEEE Transactions on Industrial Electronics*, vol. 65, no. 2, pp. 957-967, Feb. 2018, doi: 10.1109/TIE.2017.2696483.

[22] G. C. Konstantopoulos and P. R. Baldivieso-Monasterios, "State-limiting PID controller for a class of nonlinear systems with constant uncertainties," *International Journal of Robust and Nonlinear Control*, vol. 30, no. 5, pp. 1770-1787, 2020, doi: 10.1002/rnc.4853.

[23] S. Dedeoglu, G. C. Konstantopoulos and A. G. Paspatis, "Grid-Supporting Three-Phase Inverters with Inherent RMS Current Limitation Under Balanced Grid Voltage Sags," *IEEE Transactions on Industrial Electronics*, doi: 10.1109/TIE.2020.3034860.

[24] S. Dedeoglu and G. C. Konstantopoulos, "PLL-Less Three-Phase Droop-Controlled Inverter with Inherent Current-Limiting Property," *IECON 2019 - 45th Annual Conference of the IEEE Industrial Electronics Society*, Lisbon, Portugal, 2019, pp. 4013-4018, doi: 10.1109/IECON.2019.8927219.

[25] I. Sefa, S. Ozdemir, H. Komurcugil, and N. Altin, "Comparative study on Lyapunov-function-based control schemes for single-phase grid-connected voltage-source inverter with LCL filter," *IET Renewable Power Generation*, vol. 11, no. 11, pp. 1473–1482, 2017, doi: 10.1049/iet-rpg.2016.0566.

[26] H. K. Khalil, *Nonlinear systems*. Upper Saddle River, NJ: Prentice Hall, 2002.